09

Propagation of circularly polarized laser pulses in the Λ-scheme of degenerated levels

© O.M. Parshkov, I.A. Plehanova

Yuri Gagarin State Technical University of Saratov,
410054 Saratov, Russia
e-mail: oparshkov@mail.ru

Received December 21, 2023
Revised December 21, 2023
Accepted December 21, 2023

The results of a theoretical study of the joint propagation of two laser pulses in a resonant medium modeled by the Λ--scheme of inhomogeneously broadened quantum transitions between degenerate energy levels are presented. It is assumed that upon entering the medium, nanosecond pulses have circular polarization and identical intensity envelopes. For the listed estimates, the Λ--scheme formed by the levels $^3P_0$, $^3P_1^0$ and $^3P_2$ of the ^{208}Pb isotope were chosen. It is shown that in the medium there is a transfer of energy from a high-frequency pulse to a low-frequency one, which is accompanied by a change in the characteristics of the lower pulses. The magnitude and peculiarities of the distortions depend both on the intensity of relaxation processes in the Λ--scheme and on the directions of circular polarizations of the input fields. In the limiting case of the absence of relaxation and opposite direction polarizations of input radiation in, trains of picosecond subpulses arise in the medium at the trailing edges of both pulses, the maximum intensities of which significantly exceed the peak intensities of the corresponding input pulses. If the intensity of the relaxation processes is sufficiently high, such trains do not arise. In the case of identical directions of circular polarizations of the input radiations, regardless of the magnitude of the relaxation processes, the intensity envelopes of both pulses and their polarization characteristics in the medium experience significant changes at all stages of evolution.

Keywords: double resonance, electromagnetically induced transparency, selfinduced transparency.

DOI: 10.21883/0000000000

Introduction

The resonance interaction of a two-frequency laser field with quantum transitions having common energy levels, called below double resonance (DR), is widely studied due to the opportunity of its practical use. One of the first results of this study was the DR method in spectroscopy [1]. The study of electromagnetically induced transparency (EMIT) [2–4], a special case of DR, opened the way for the creation of optical memory systems [3] and quantum communications [3,5,6], systems quantum information [2–4], devices for precise measurement of magnetic fields [7], devices for precise time measurement [8]. The EMIT phenomenon allows to create large optical nonlinearities [4,9] and to realize radiation amplification without population inversion [10]. The features of this phenomenon have been studied in strongly correlated quantum gases [11], in the radio range [12], on impurities in photonic crystals [13], near nanofibers [14], in the presence of angular orbital momentum of the test field [15].

Many practical applications of DR are based on the properties of pulses of interacting fields to propagate in a medium over significant distances without significant distortion of their energy and polarization characteristics [2–6]. Theoretical study led to the description of such impulse structures of DR as simultons [16], Raman solitons [17], adiabatons [18], matched pulses [19]. Experiments to observe these pulse structures required satisfying conditions that are difficult to implement in practice. Therefore, the main attention in the study of DR has shifted to the region of the EMIT phenomenon when the conditions of the adiabatic approximation are met [20]. The use of the adiabatic approximation assumes a slow change in the parameters of the interacting pulses and is not able to describe the rapid oscillations of their intensities that occur in the medium. The opportunity of the occurrence of such oscillations was discovered in theoretical work [21]. The model used in [21] is limited to the Λ- circuit of simple energy levels and does not take into account the heterogeneous broadening of quantum transition lines. The model also does not take into account the opportunity of changing polarization states and phase modulation (PM) of pulses in the medium and assumes the absence of relaxation processes.

This work presents the results of a numerical analysis of DR in an open Λ- circuit formed by the $^3P_0$, $^3P_1^0$ and $^3P_2$ levels of the ^{208}Pb isotope, in which

EMIT of circularly polarized laser fields was experimentally observed [22,23]. The choice of such an Λ-circuit is due to the absence of a hyperfine structure of the energy levels of the ^{208}Pb isotope. Calculations were carried out in the plane wave approximation, taking into account the degeneracy of the energy levels of the Λ- circuit, the heterogeneous broadening of the spectral lines of quantum transitions, taking into account the possibility of changes in polarization states and the emergence of PM interacting fields. It is assumed that both interacting pulses at the entrance to the medium have intensity envelopes that are identical in shape, peak value and duration. Let us note that the work [24] presents the results of a numerical analysis of the double resonance process in the considered Λ- circuit for the case when the duration of the input high-frequency (HF) pulse is significantly less than the duration of the input low-frequency (LF) pulse.

1. Problem formulation

The Λ- circuit under study consists of a simple lower level ^{3}P$_0$, a fivefold degenerate middle ^{3}P$_2$ and a threefold degenerate upper ^{3}P$_1^0$ levels, respectively. Let us note that below the average level ^{3}P$_2$ is the level ^{3}P$_1$ (Fig. 1), connected to the upper and middle levels Λ- of the circuit by electrodipole moments. Relaxation processes connecting the excited levels Λ- of the circuit with the level ^{3}P$_1$ lead to a decrease in the total number of atoms at its levels and an additional broadening of the lines of quantum transitions. It is natural to call such an Λ- circuit open, as opposed to the case of a closed Λ- circuit, in which all relaxation processes connect only the levels of resonance transitions.

Let us choose an orthonormal basis ϕ_k $(k = 1, 2 \ldots 9)$ consisting of the general eigenfunctions of the Hamiltonian, the square of the angular momentum and the projection of the angular momentum onto the axis z to describe the states included in the Λ- circuit of the atom ^{208}Pb. Function Φ_1 refers to level ^{3}P$_0$, functionϕ_k $(k = 5, 6, \ldots 9)$ — to states of level ^{3}P$_2$ (P $= -2, -1, 0, 1, 2$), functions ϕ_k $(k = 2, 3, 4)$ — to states of level ^{3}P$_1^0$ (Fig. 1). Let D_1 and D_2 — the reduced dipole moments of the HF transition ^{3}P$_0 \to {}^3$P$_1^0$ and the LF transition ^{3}P$_2 \to {}^3$P$_1^0$, respectively, and let ω_1 and ω_2 $(\omega_1 > \omega_2)$ — the frequencies of these transitions for an atom at rest. We take into account the heterogeneous broadening of spectral lines by introducing the Gaussian density $g(\omega_1')$ of the frequency distribution ω_1' of transitions ^{3}P$_0 \to {}^3$P$_1^0$ of moving atoms:

$$g(\omega_1') = (T_1/\sqrt{\pi}) \exp\left[-T_1^2(\omega_1' - \omega_1)^2\right],$$

where T_1 — time parameter of heterogeneous broadening.

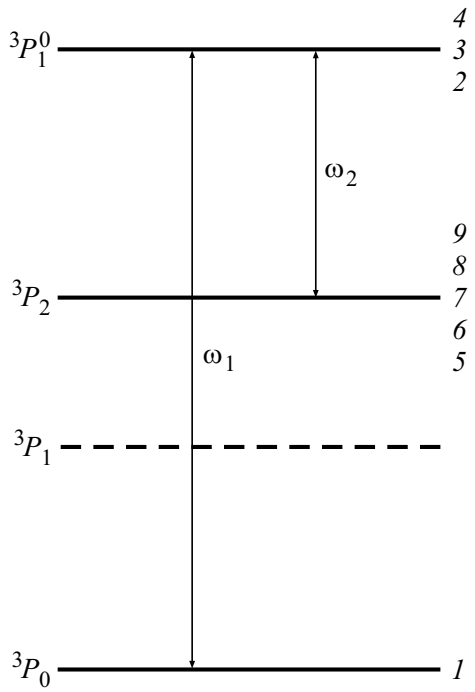

Figure 1. Energy levels of the Λ circuit (solid lines), level not included in the Λ circuit (dashed line); numbers to the right of the level lineΛ circuit numbers of states belonging to this level, according to the theoretical model.

Let us write the electric field strength in the medium in the form: $\mathbf{E} = \mathbf{E}_1 + \mathbf{E}_2$,

$$\mathbf{E}_l = \mu_l(\mathbf{e}_x E_{xl} \cos(\omega_l t - k_l z + \delta_{xl})$$

$$+ \mathbf{e}_y E_{yl} \cos(\omega_l t - k_l z + \delta_{yl})\big], \quad l = 1, 2. \tag{1}$$

Here $\mathbf{E}_l$ and ω_l — electric field strength and carrier frequency of radiation; $\mathbf{e}_x, \mathbf{e}_y$ — axis unit vectors x, y; E_{xl}, E_{yl} — amplitudes; δ_{xl}, δ_{yl} $(-\pi \le \delta_{xl}, \delta_{yl} \le \pi)$ — phase additives x-, y-field components describing their PM;

$$\mu_l = \hbar\sqrt{2l+1}/(|D_l|T_1);$$

$$k_l = \omega_l/c.$$

At $l = 1$, formula (1) describes HF radiation resonant with the transition ^{3}P$_0 \to {}^3$P$_1^0$ between the ground and upper levels. At $l = 2$, formula (1) describes HF radiation resonant with the transition ^{3}P$_2 \to {}^3$P$_1^0$ between the ground and upper levels. Let's introduce new independent variables s and w:

$$s = z/z_0, \quad w = (t - z/c)/T_1,$$

putting $z_0 = 3\hbar c/(2\pi N|D_1|^2 T_1 \omega_1$, N — concentration of atoms. Using Maxwell's equations and Schrödinger's equations, we obtain in the first approximation of the slow

envelope method, the following system of equations:

$$\frac{\partial f_1}{\partial s} = \frac{i}{\sqrt{\pi}} \int_{-\infty}^{+\infty} c_1 c_2^* \exp(-\varepsilon_1^2) d\varepsilon_1, \qquad \frac{\partial f_2}{\partial s} = -\frac{i}{\sqrt{\pi}} \xi \int_{-\infty}^{+\infty} (c_4^* c_9 + c_2^* c_7) \exp(-\varepsilon_1^2) d\varepsilon_1,$$

$$\frac{\partial g_1}{\partial s} = -\frac{i}{\sqrt{\pi}} \int_{-\infty}^{+\infty} c_1 c_4^* \exp(-\varepsilon_1^2) d\varepsilon_1, \qquad \frac{\partial g_2}{\partial s} = \frac{i}{\sqrt{\pi}} \xi \int_{-\infty}^{+\infty} (c_2^* c_5 + c_4^* c_7) \exp(-\varepsilon_1^2) d\varepsilon_1,$$

$$\frac{\partial c_1}{\partial w} = -i(f_1 c_2 - g_1 c_4), \qquad \frac{\partial c_2}{\partial w} + i\varepsilon_1 c_2 = -\frac{i}{4}(f_1^* c_1 + g_2^* c_5 + f_2^* c_7) - \gamma c_2,$$

$$\frac{\partial c_4}{\partial w} + i\varepsilon_1 c_4 = \frac{i}{4}(g_1^* c_1 + g_2^* c_7 + f_2^* c_9) - \gamma c_4, \qquad \frac{\partial c_5}{\partial w} + i(\varepsilon_1 - \varepsilon_2) c_5 = -i g_2 c_2,$$

$$\frac{\partial c_7}{\partial w} + i(\varepsilon_1 - \varepsilon_2) c_7 = \frac{i}{6}(f_2 c_2 - g_2 c_4), \qquad \frac{\partial c_9}{\partial w} + i(\varepsilon_1 - \varepsilon_2) c_9 = i f_2 c_4. \tag{2}$$

When writing equations (2), the following notation was used:

$$\varepsilon_1 = (\omega_1' - \omega_1) T_1/2, \ \ \varepsilon_2 = \beta\varepsilon_1, \ \ \beta = \omega_2/\omega_1,$$

$$\xi = 0.6\beta |D_2/D_1|^2,$$

$$c_1 = \frac{|D_1|}{2D_1^*}\,\bar{c}_1, \ \ c_2 = \bar{c}_2, \ \ c_4 = \bar{c}_4,$$

$$c_{5,9} = \frac{|D_2|}{2D_2}\,\bar{c}_{5,9}, \ \ c_7 = \frac{\sqrt{6}}{2}\,\frac{|D_2|}{D_2}\,\bar{c}_7,$$

$\bar{c}$, $k = 1, 2, 4, 5, 7, 9$ — state population probability amplitude k. (Due to the $\Delta M = \pm 1$ selection rules, the $\bar{c}_k$, $k = 3, 6, 8$ amplitudes are not included in the system (2).) The terms $-\gamma c_2$, $-\gamma c_4$ are phenomenologically introduced into the equations to take into account the relaxation decay of the states of the upper level $^3P_1^0$ of the Λ- circuit under consideration. Below, the value γ is called the relaxation parameter. Let us note that the middle level of this scheme is metastable.

In many studies, to describe the response of a medium to an electromagnetic field, standard density matrix equations are used with the introduction of terms that describe Markov-type relaxation processes. A rigorous justification for this method is given, for example, in [25] and requires the absence of degeneracy of energy levels. This condition is obviously not satisfied for the Λ- circuit under consideration. Therefore, the use of the standard density matrix method to find its 45 independent matrix elements is inappropriate in our case. We use the equations for the probability amplitudes of the populations of the states of the degenerate Λ- circuit, which follow from the Schrödinger equation, by including phenomenologically relaxation terms in the equations for the probability amplitudes of the states of the $^3P_1^0$ level. This method of taking into account relaxation also takes into account the relaxation damping of the polarization of the medium and the decrease in the number of particles at the levels Λ- of the scheme, associated with the transition of atoms ^{208}Pb to the level $^3P_1$. There are quite a lot of works (see, for example, [10,19]) in which the method of phenomenological introduction of relaxation into the Schrödinger equation was used to describe the evolution of radiation in a resonance medium.

The following parameters of the polarization ellipse (PE) of the HF ($l = 1$) and LF ($l = 2$) fields are used below: a_l— semi-major axis of the EP, measured in units μ_l, α_l ($0 \le \alpha_l \le \pi$) — angle between it and the axis x, γ_l — compression parameter ($-1 \le \gamma_l \le 1$). The modulus γ_l is equal to the ratio of the minor axis of the electron beam to its major axis, $\gamma_l < 0$ ($\gamma_l > 0$) in the case of right (left) elliptical polarization. With circular polarization, the value α_l is not defined and is conventionally assumed to be equal to -0.1. Dimensionless intensities I_l of HF ($l = 1$) and LF ($l = 2$) fields, measured in units of $c\mu_1^2/(8\pi)$, are also used.

When solving system (2), it is assumed that at the initial moment of time ($w = 0$) only the lower level $^3P_0$ Λ- of the circuit is populated. The boundary conditions are formulated by specifying the quantities a_l, α_l, γ_l, δ_{xl} as functions of the variable w on the input surface of the medium ($s = 0$):

$$a_1(0, w) = a_{10}\,\mathrm{sech}[(w - 1000)/100], \ \ \alpha_1(0, w) = -0.1,$$

$$\gamma_1(0, w) = \gamma_{10}, \ \ \delta_{x1}(0, w) = 0, \tag{3}$$

$$a_2(0, w) = a_{20}\,\mathrm{sech}[(w - 1000)/100],$$

$$\alpha_2(0, w) = -0.1, \ \ \gamma_2(0, w) = 1, \ \ \delta_{x2}(0, w) = 0. \tag{4}$$

Here $a_{10} = 2.828$, $a_{20} = 4.910$, and the value γ_{10} will be assumed to be equal to -1 or $+1$. Formulas (3), (4) describe HF and LF pulses with intensity envelopes in the form of an inverse hyperbolic cosine with a duration of 100 units of time w. The peak intensities of the input pulses are the same: $I_l = 16$, $l = 1, 2$, and they are deprived of PM.

According to [26], for the selected transitions ^{208}Pb in the formulas $\beta = 0.7$, $\xi = 2.11$. In case of $T = 1050$ K we

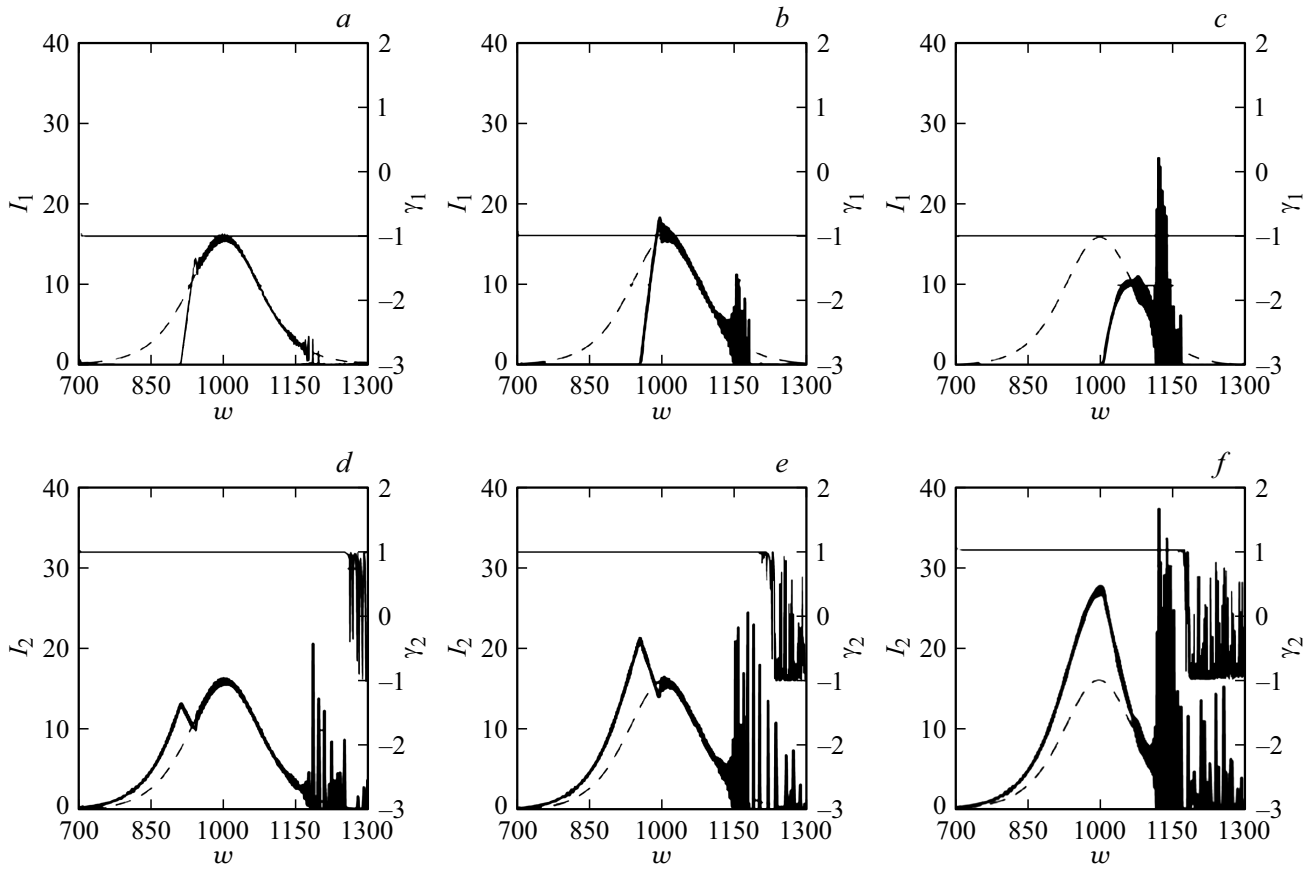

Figure 2. Evolution of the quantities I_1 (thick lines), γ_1 (thin lines) and I_{10} (dashed) at $s = 500$ (a), 1000 (b), 2000 (c); evolution of the quantities I_2 (thick lines), γ_2 (thin lines) and I_{20} (dashed) at $s = 500$ (d), 1000 (e) and 2000 (f).

have $T_1 = 1.6 \cdot 10^{-10}$ s. Choosing saturated pairs ^{208}Pb for estimation and using the data [27], we find at the same temperature $N = 2.8 \cdot 10^{14}\,\mathrm{cm}^{-3}$ and $z_0 = 0.004$ cm. Note that the value z_0 strongly depends on temperature, while the value T_1 practically does not change in the temperature range $T = 950-1300$ K. The dimensionless intensity I_l is related to the dimensional value $\tilde{I}_l$ of this quantity by the relation $\tilde{I}_l = 1.3 I_l\,\mathrm{kW/cm}^2$, and its peak value at the entrance to the medium is close to $20\,\mathrm{kW/cm}^2$. This was approximately the intensity of the LF pulses in the experiments [22,23]. The duration of each input pulse is approximately 30 ns. Here and below, pulse duration is measured at half peak intensity.

To estimate the relaxation parameter γ we use the relation $\gamma = T_1/(2\pi)$, τ — lifetime of the $^3\mathrm{P}_1^0$ level. At a sufficiently low concentration of atoms ^{208}Pb ($N \ll 10^{16}\,\mathrm{cm}^{-3}$) τ is the time of radiative decay of states of this level. Using [26], we then have $\tau \cong 5.6$ ns. At large values of N, the main contribution to the relaxation of states of the $^3\mathrm{P}_1^0$ level will be made by collisional processes, and the value of τ can become significantly less than the radiation-induced decay time of states of this level. Using the data from the work [27], it can be shown that in saturated vapors ^{208}Pb the value $N = 10^{16}\,\mathrm{cm}^{-3}$ is achieved at $T = 1280$ K.

2. Calculation results

2.1. Opposite directions of circular polarizations of input pulses

2.1.1. Absence of relaxation. Let us first consider the hypothetical case of the complete absence of relaxation processes. This situation is realized when the duration of the radiation pulses is significantly less than the relaxation times of all quantum transitions. In our case, the radiation-induced lifetime τ of the $^3\mathrm{P}_1^0$ level is 5.6 ns, and formulas (3) and (4) define pulses of much longer duration, so this situation does not occur. However, its study is useful for the physical interpretation of the results of calculations that take into account relaxation processes. The absence of relaxation is characterized by the condition $\tau = +\infty$ or $\gamma = 0$, where γ — the relaxation parameter introduced previously.

In the formulas (3) we assume $\gamma_{10} = -1$. This means that the HF pulse at the entrance to the medium is circularly polarized to the right, and the LF pulse is circularly polarized to the left. Figure 2 shows graphs of intensities I_l and compression parameters γ_l, $l = 1, 2$, for three distance values s. The dashed line in Fig. 2 shows the intensity envelope I_{l0}, $l = 1, 2$ of the reference pulse. The reference pulse below refers to the input pulse propagating in empty

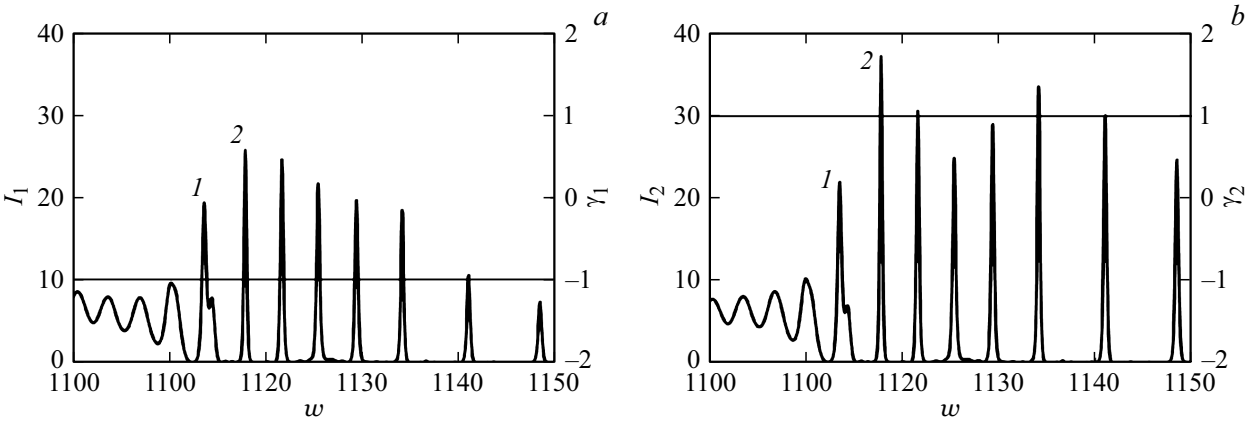

Figure 3. Evolution of the values I_l and γ_l, $l = 1, 2$ at $s = 2000$ for HF (a) and LF (b) pulses; I_l — thick lines, γ_l — thin lines.

space. Fig. 2 shows that with increasing distance s, energy is transferred from the HF pulse to the LF radiation pulse. In this case, trains of subpulses appear at the trailing edge of the pulses, which cannot be resolved on the scale of the figures. In the case of an HF pulse (Fig. 2, a–c) the parameter is $\gamma_1 = -1$ at all distances s. Moreover, for all s, as the calculation shows, $\alpha_1 = -0.1$. This means that in the HF medium the pulse remains circularly polarized to the left. The calculation also showed that for all s the HF pulse is devoid of PM. Further such trains of subpulses are referred to as regular.

Trains of subpulses at the trailing edge of the LF pulse (Fig. 2, d–f) can be conditionally divided into two groups. Regular trains, as above, are trains with a constant value $\gamma_2 = 1$. Regular trains are represented by a set of subpulses, polarized in a circle to the right and, as calculations show, devoid of PM. Let us n that regular trains of subpulses of HF and LF radiation for all s are located in the same time region. In addition, at the trailing edge of the LF pulse there are irregular trains of subpulses. In the region of irregular trains, the value of γ_2 changes rapidly (Fig. 2, d–f). Variables in the region where irregular trains are located are, as calculation shows, the values α_2 and δ_{x2}. This means that the radiation of an irregular train of subpulses has a variable type of polarization and has PM.

Fig. 3 shows fragments of regular trains of subpulses of HF (Fig. 3, a) and LF (Fig. 3, b) radiations at $s = 2000$. Let us note that each HF subpulse is located in the same space-time region with a certain LF field subpulse, and the I_1 and I_2 curves of this pair of subpulses are similar. Such pairs form, for example, subpulses *1* or *2* in Fig. 3. This means that the subpulses of each pair interact with each other. The values of γ_1 and γ_2 in Fig. 3 show that the HF field subpulses are circularly polarized to the right, and the LF radiation subpulses are polarized to the left. The peak intensity of the subpulse *2* in Fig. 3, a is 33 kW/cm^2, and that of the subpulse *2* in Fig. 3, b — 48 kW/cm^2 ($T = 950$–1300 K). These values exceed the peak intensities of the input pulses. The duration of the subpulses is approximately 50 ns, and the average distance between them is approximately 700 ps.

2.1.2. Radiation-induced relaxation. In the case of a low concentration of atoms ^{208}Pb, the relaxation process is associated with the radiation-induced (spontaneous) decay of quantum states. In our model, such decays are taken into account by introducing the time τ of spontaneous decay of the level $^3P_1^0$: $\tau = 5.6$ ns, from which it follows that with $T = 1050$ K the parameter is $\gamma = 1.5 \cdot 10^{-2}$. Figure 4 shows graphs of intensities I_l and compression parameters γ_l, $l = 1, 2$, for $s = 2000$. The dashed line in Fig. 4 shows the intensity envelope I_{l0}, $i = 1, 2$ of the reference pulse. The graphs of the characteristics of HF and LF pulses in the medium differ from those shown in Fig. 2, c and f by a decrease in the intensity of trains of regular subpulses (irregular trains of low-frequency pulses are now absent). The pulses of both radiations at all distances s are circularly polarized and, as calculations show, are devoid of PM.

Fig. 5 shows fragments of regular trains of subpulses of HF (Fig. 5, a) and LF (Fig. 5, b) radiations at $s = 2000$. Subpulses *1*, as well as subpulses *2* (Fig. 5), have similar intensity envelopes that simultaneously reach peak values. Graphs of the values γ_1 and γ_2 indicate that the radiation from the trains is circularly polarized in the same direction as the corresponding input pulses. According to calculations, the subpulses of both fields are devoid of PM, so these trains should be classified as regular. Comparison of graphs in Fig. 3, a and 5, a, as well as graphs in Fig. 3, b and 5, b shows that the subpulses of a regular train in the absence of relaxation are much more intense than in the presence of radiation-induced decay.

2.1.3. Shock relaxation. If the concentration of atoms ^{208}Pb exceeds 10^{16} cm^{-3}, collisional processes, for example, broadening by self-pressure, will make a significant contribution to relaxation. Let us assume that $\gamma = 3.0 \cdot 10^{-2}$, which is twice as much as in the case of radiation-induced relaxation. Figure 6 shows graphs of intensities I_l and compression parameters γ_l, $l = 1, 2$, for three distance values s. The dashed line in Fig. 6 shows

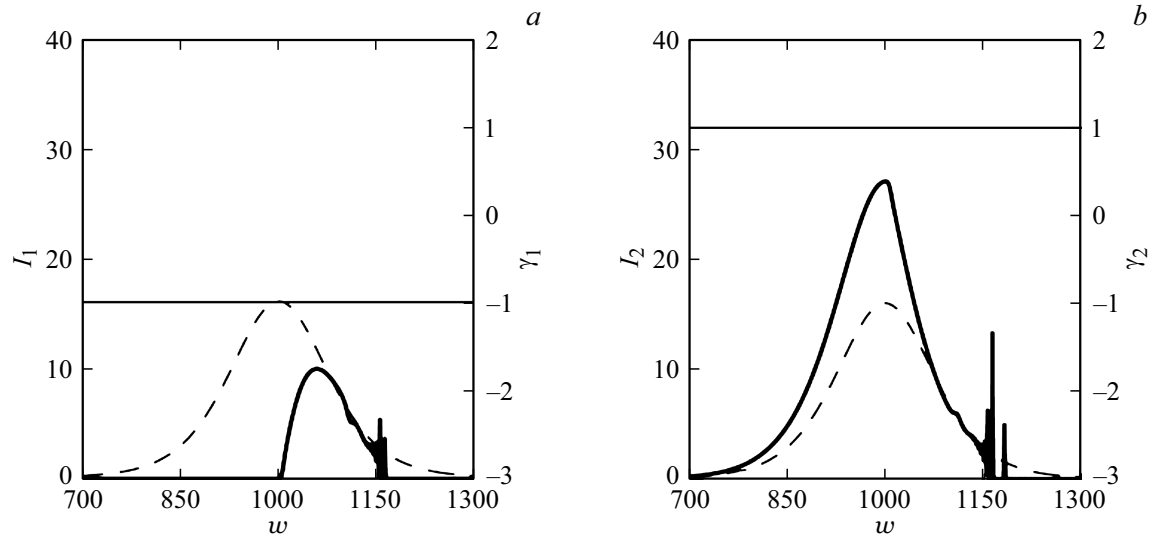

Figure 4. Evolution of the values I_l (thick lines), γ_l (thin lines) and I_{l0} (dashed) at $s = 2000$, at $l = 1$ (a) and 2 (b).

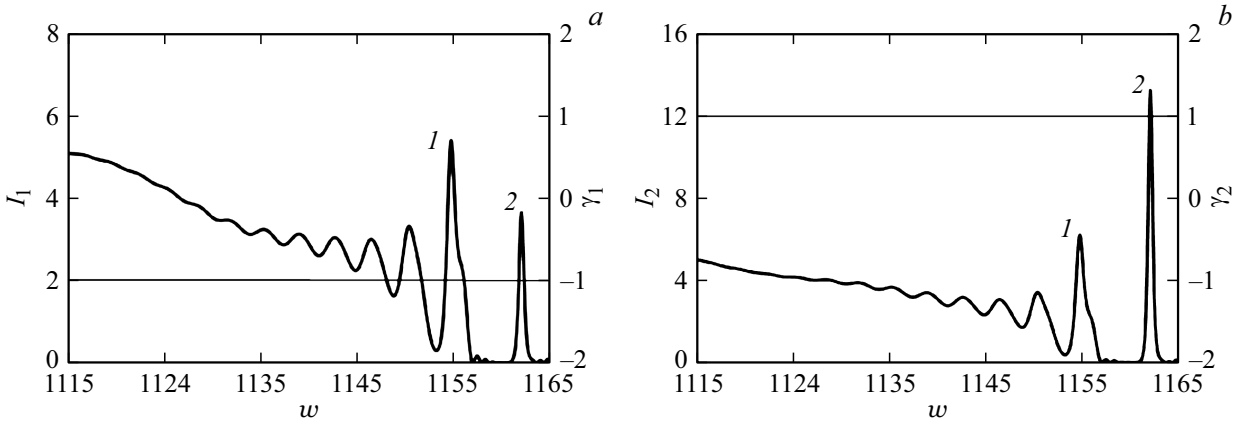

Figure 5. Evolution of the values I_l and γ_l, $l = 1, 2$ at $s = 2000$ for HF (a) and LF (b) pulses; I_l — thick lines, γ_l — thin lines.

the intensity envelope I_{l0}, $l = 1, 2$ of the reference pulse. Fig. 6 shows that in the presence of sufficiently strong relaxation processes, trains of subpulses do not arise at the trailing edges of the pulses. The values of the parameters γ_l, $l = 1, 2$, during pulse propagation, remain unchanged and equal to their values for $s = 0$. The calculation shows that the same properties characterize the values of the quantities α_l and δ_{xl}, $l = 1, 2$. Consequently, both pulses in the medium remain circularly polarized and lack PM.

Let us denote the total energy of the electromagnetic field transferred by a pulse through a unit cross-sectional area located at a distance of s from the entrance ($s = 0$) to the resonance medium by $\mathrm{W}(s)$. The value $\mathrm{W}(s)/\mathrm{W}(0)$ characterizes the relative change in the pulse energy during propagation. Figure 7 shows graphs of the dependence of the value $\mathrm{W}(s)/\mathrm{W}(0)$ for calculations in the absence of relaxation and in the presence of shock relaxation. Let us note the coincidence of the curves for HF radiation pulses, which means the equality of their energies at all distances. Taking this into account and comparing the I_1 curves in Figs. 2 and 6, we come to the conclusion that relaxation processes lead to the conversion of the energies of trains of subpulses of the HF field into the energy of a monopulse with a bell-shaped intensity envelope. The same conclusion is true for a pulse of LF radiation. However, as Fig. 7 shows, the energy of a LF pulse in the presence of relaxation increases with distance somewhat more slowly than in its absence.

2.2. Similar directions of circular polarizations of input pulses

Let us assume $\gamma_{10} = 1$. This means that the input pulses are circularly polarized to the left.

2.2.1. Absence of relaxation. This hypothetical situation is illustrated in Fig. 8, which shows graphs of the values I_l and γ_l, $l = 1, 2$, at $s = 600$. Fig. 8 shows

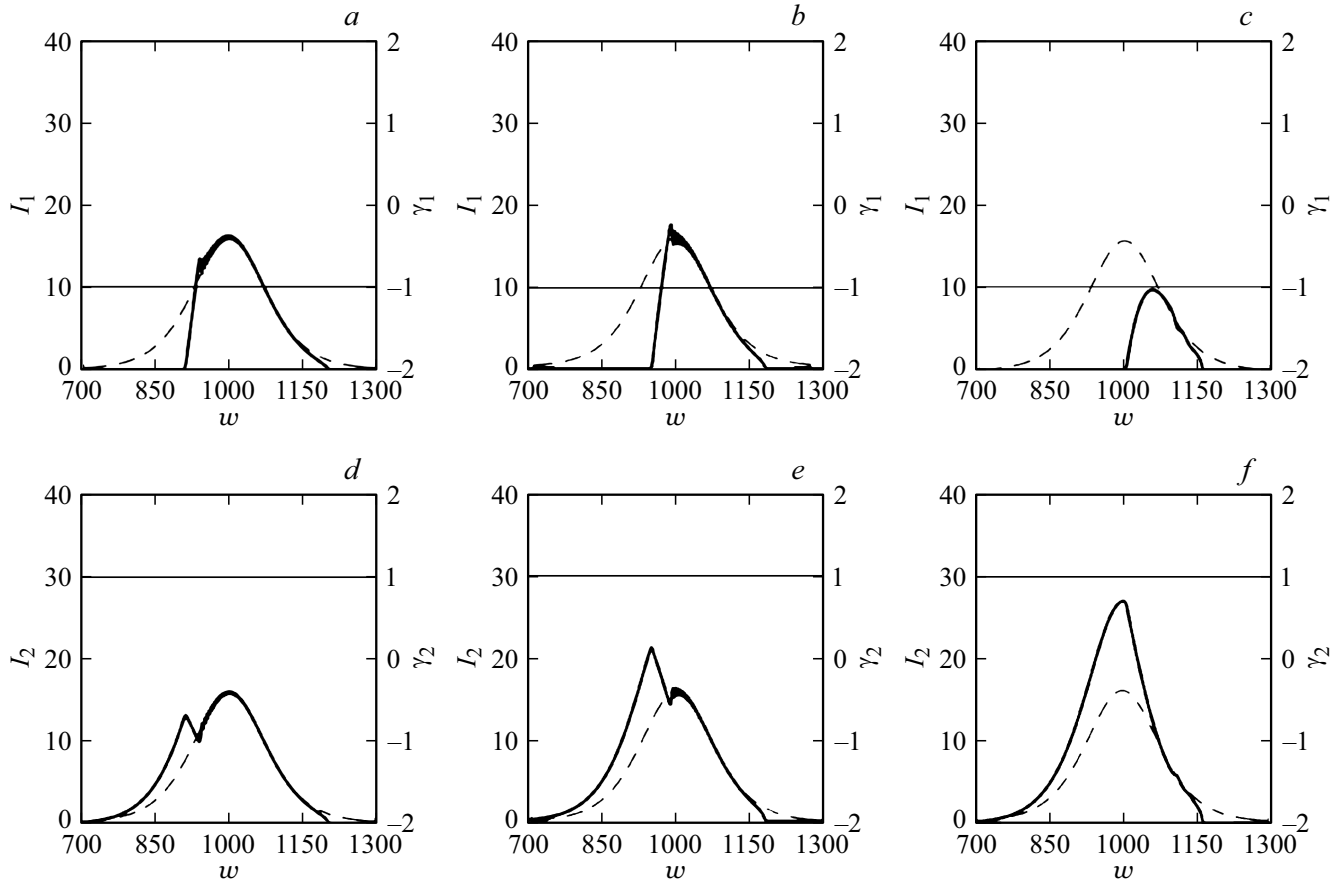

Figure 6. Evolution of the quantities I_1 (thick lines), γ_1 (thin lines) and I_{10} (dashed) at $s = 500$ (a), 1000 (b), 2000 (c); evolution of the quantities I_2 (thick lines), γ_2 (thin lines) and I_{20} (dashed) at $s = 500$ (d), 1000 (e) and 2000 (f).

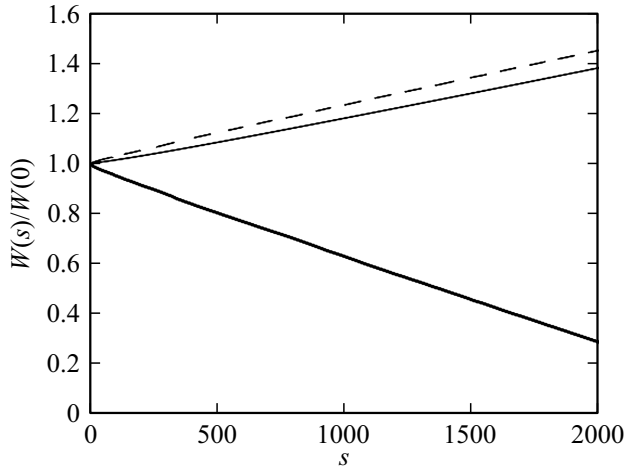

Figure 7. Value W(s)/W(0) for a HF pulse in the presence and absence of relaxation (thick line), for a LF pulse in the presence of relaxation (thin line) and in the absence of relaxation (dashed line).

that at this distance the intensity envelopes have a chaotic structure both at the trailing and leading edges of the pulses. Meanwhile, the compression parameters of γ_l are variable at all stages of the evolution of radiation. The calculation shows that the quantities α_l and δ_{xl}. also have the same property. Consequently, pulses in the medium have an alternating type of polarization and exhibit PM. Let us note that in the case of different circular polarizations of input pulses in the absence of relaxation, the quantities γ_l, α_l and δ_{xl}, $l = 1, 2$, oscillate only in the region of irregular trains at the trailing edge of the LF pulse, even at $s = 2000$ (Fig. 2, d–f).

2.2.2. Shock relaxation. As when reviewing the influence of shock relaxation in the case of input pulses with different directions of circular polarization, we assume $\gamma = 3.0 \cdot 10^{-2}$. Figure 9 shows graphs of intensities I_l and compression parameters γ_l, $l = 1, 2$, for three distance values s. Figure 9 shows that the presence of shock relaxation does not lead to the formation of pulses with a bell-shaped intensity envelope. In addition, unlike the case of opposite directions of circular polarization of input pulses, the parameters γ_l, $l = 1, 2$ are not constant. Calculations show that the values of α_l and δ_{xl} change over time as well. Thus, both pulses in the medium have an alternating type of polarization and exhibit PM.

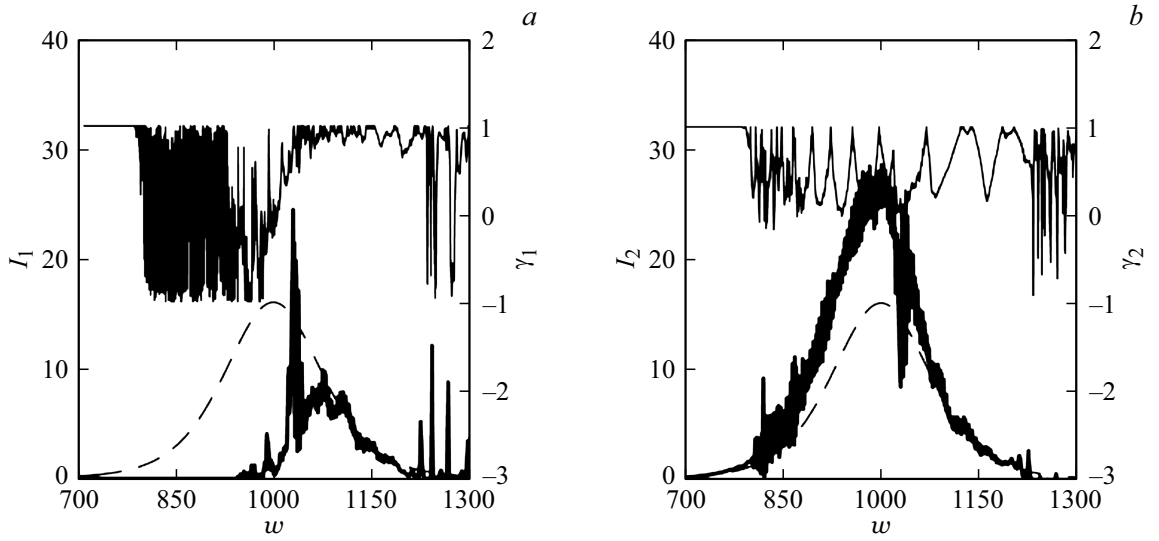

Figure 8. Evolution of the values I_l (thick lines), γ_l (thin lines) and I_{l0} (dashed) at $s = 600$, for $l = 1$ (a) and 2 (b).

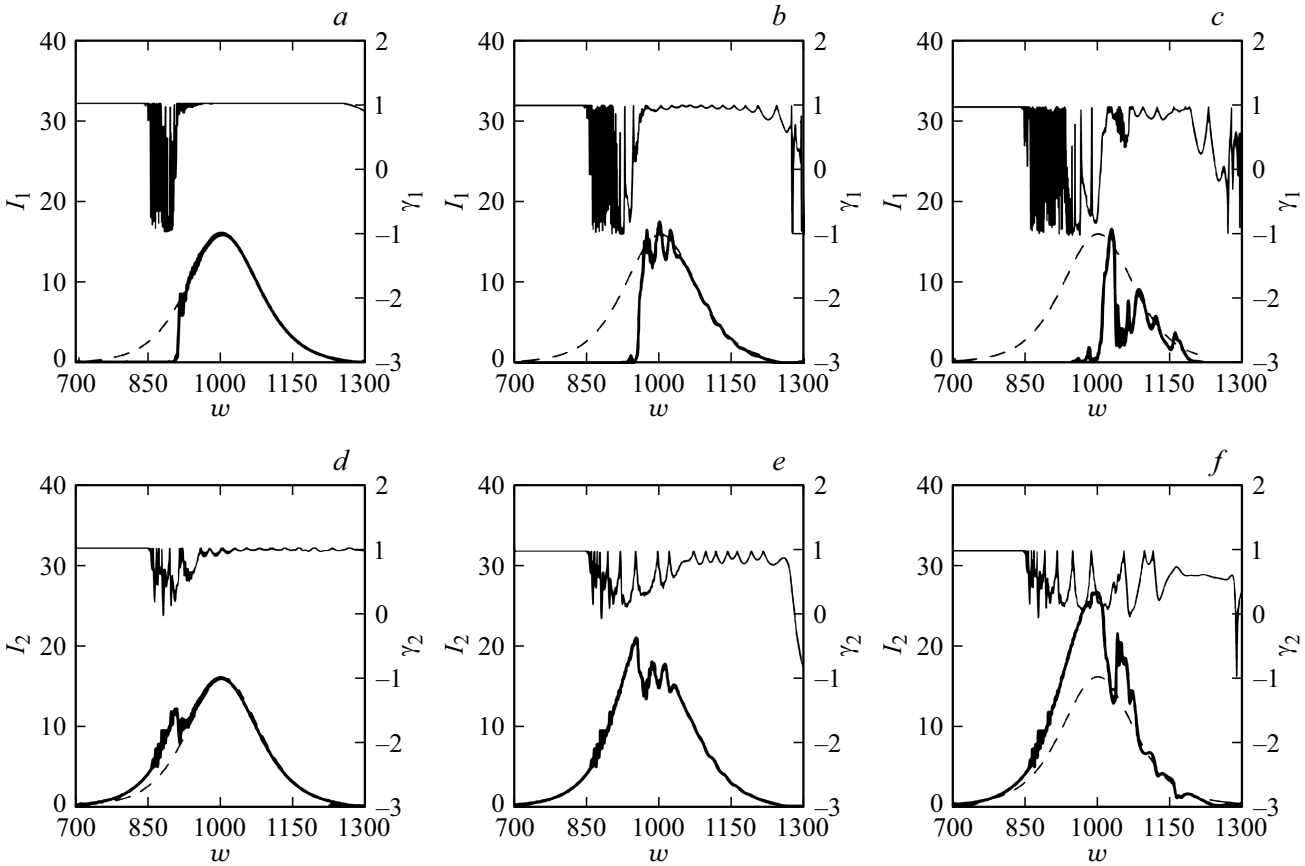

Figure 9. Evolution of the quantities I_1 (thick lines), γ_1 (thin lines) and I_{10} (dashed) at $s = 150$ (a), 300 (b), 600 (c); evolution of the quantities I_2 (thick lines), γ_2 (thin lines) and I_{20} (dashed) at $s = 150$ (d), 300 (e) and 600 (f).

3. Discussion

The above-described features of pulse propagation can be interpreted as a result of the manifestation of two effects. The first of them is the EMIT effect, and the second is the effect of self-induced transparency (SIT) [28]. In the presence of LF radiation, thanks to EMIT, the absorption of HF radiation associated with direct single-photon excitation of states of the upper level of the Λ- circuit is completely or partially eliminated. The SIT effect can lead to the decay

of the input RF pulse into a set of subpulses called 2π pulses [28] due to the single-photon resonance excitation of these states. The effectiveness of EMIT decreases with decreasing intensity of LF radiation. To increase the efficiency of the SIT phenomenon, it is required that the duration of exposure of the atom to radiation is significantly less than the time of irreversible relaxation of the resonance quantum transition.

Let us stop on the case of opposite circular polarizations of input pulses and the complete absence of relaxation processes ($\tau = +\infty$). Fig. 2 shows that as the HF field pulse propagates, it shifts toward the trailing edge of the LF field pulse. This circumstance is explained by the known fact of a decrease in the speed of propagation of the HF pulse due to the EMIT phenomenon. In this case, part of the trailing edge of the HF pulse appears in the region of the weak field of the trailing edge of the LF pulse. In this case, the efficiency of the EMIT decreases, and the SIT phenomenon begins to play a major role in the process of evolution of this part of the trailing front. It can be assumed that the trains of subpulses at the trailing edge of the HF pulse (Fig. 2, a–c) consist of the forming 2π SIT pulses.

This circumstance is confirmed by the following considerations. Using the results of the work [28], it can be shown that for a circularly polarized2π pulse at the frequency of HF radiation the condition $\tau_1\sqrt{I_{1m}/2} = 8$ should be satisfied, where I_{1m} — the peak value of its intensity, τ_1 — pulse duration according to $e^{-2}I_{1m}$ level. For the pulse marked with the number *2* in Fig. 3, a, the calculation gives $\tau_1\sqrt{I_{1m}/2} = 8.9$. In the case of the last pulse in Fig. 3, a we have $\tau_1\sqrt{I_{1m}/2} = 5.8$. Consequently, the intensity envelopes of the train subpulses are close in shape to the intensity envelopes of the2π SIT pulses.

The SIT phenomenon is accompanied by a significant change in the populations of the states of the upper energy level of the Λ- circuit, up to the creation of population inversion between its upper and middle levels in the region where RF radiation subpulses are located. Processes of stimulated emission at the frequency of a LF field lead to the appearance of trains of subpulses at the trailing edge of the pulse of this field. Meanwhile, an energy exchange occurs between each HF field subpulse and a LF field subpulse located in the same space-time region. Its presence does not allow HF subpulses to turn into full-fledged 2π pulses. In particular, the propagation speeds of the maximum values of the intensity envelopes of these subpulses are much greater than those prescribed by the SIT theory [28] and even exceed the speed of light in vacuum. This circumstance does not contradict the well-known postulate of the theory of relativity and means that the peak intensity value in the case under consideration is not a signal from the point of view of this theory [29].

If the time τ of irreversible relaxation is sufficiently short compared to the duration of the trailing edge of the RF pulse, then the effectiveness of the SIT phenomenon decreases or disappears completely. Therefore, in the case of purely radiation-induced decay of the upper level of the Λ- circuit (Fig. 4), the intensity of the trains is significantly less than in the absence of relaxation (Fig. 2), and in the case of shock relaxation (Fig. 6) such trains do not arise at all.

Let us move on to the case of identical directions of circular polarizations of input pulses. Calculations show (Figs. 8 and 9) that at relatively small distances s the pulse intensity envelopes are significantly distorted. Both in the presence and absence of relaxation, the state of polarization of both radiations changes in time and space, and both pulses, as calculations show, have PM. The reason for this is the weakening of the efficiency of the EMIT phenomenon upon transition from opposite to identical directions of circular polarizations of input pulses.

Indeed, let us consider the initial stage of the interaction of pulses, which occurs near the input surface. According to the selection rules $\Delta M = \pm 1$, in the case of opposite directions of circular polarizations of input pulses at this stage, quantum transitions between the states ${}^3P_0(M = 0)$, ${}^3P_1^0(M = 1)$ and ${}^3P_2(M = 2)$ lower, upper and middle energy levels. For the same directions of circular polarizations of input pulses, such states are ${}^3P_0(M = 0)$, ${}^3P_1^0(M = -1)$ and ${}^3P_2(M = 0)$, correspondingly. In both cases, the magnitudes of the dipole moments of transitions between the states of the lower and upper energy levels are similar. However, in the first case, the squared modulus of the dipole moment of the transition between the states of the middle and upper levels is five times greater than in the second case [26]. According to the EMIT [4] theory, the depth of the RF penetration pulse into the medium decreases with decreasing the square of the dipole moment of the transition between excited states of Λ- circuit. Meanwhile, the degree of distortion in the environment of the energy, polarization and phase characteristics of both radiation increases.

Conclusion

Calculations have shown that the evolution of pulses propagating together in a medium modeled by the Λ-circuit of degenerate energy levels and circularly polarized on the input surface of this medium is determined by the competition of the EMIT and SIT phenomena. The degree of influence of each of these effects depends on the intensity of relaxation processes occurring in the Λ- circuit and the directions of circular polarizations at the entrance to the medium. If relaxation is absent or weak enough, and the input pulses are polarized in opposite directions, then the largest part of each pulse evolves under the influence of EMIT. The intensity envelopes of these parts of the pulses have a smooth bell-shaped shape. However, at the trailing edge of each of them, the influence of EMIT practically disappears, and the evolution of the radiation is determined by the SIT process. In view of this, trains of ultrashort subpulses appear at the trailing edges of the pulses. If the input laser radiation was devoid of PM, then in the medium its radiation remains circularly polarized and devoid of PM.

If the relaxation processes are sufficiently intense, then the SIT phenomenon does not occur and the indicated pulse trains are absent.

In the case of different directions of circular polarization of input pulses, the influence of EMIT on the process of their propagation in the medium is significantly reduced. As a result, the shapes of pulse intensity envelopes are significantly distorted at distances that are small compared to the case of opposite polarizations of input radiation. Pulses in the medium have a variable polarization structure and obtain PM.

Conflict of interest

The authors declare that they have no conflict of interest.

References

[1] V. Demtreder. *Sovremennaya lazernaya spektroskopiya*, per. s angl. pod red. L.A. Mel'nikova (Izdat. dom Intellekt, Dolgoprudnyy, 2014) (in Russian).
[2] S.E. Harris. Phys. Today, **50** (6), 36 (1997).
[3] M.D. Lukin. Rev. Mod. Phys., **75** (2), 457 (2003).
[4] M. Fleischhauer, A. Imamoğlu, J.P. Marangos. Rev. Mod. Phys., **77** (2), 633 (2005).
[5] L.-M. Duan, M.D. Lukin, J.I. Cirac, P. Zoller. Nature (London), **414**, 413 (2001).
[6] A. Sinatra. Phys. Rev. Lett., **97** (25), 253601 (2006).
[7] M. Martinalli, P. Valente, H. Failache, D. Felinto, L.S. Cruz, P. Nussenzveig, A. Lezama. Phys. Rev. A, **69** (4), 043809 (2004).
[8] A. Godone, S. Micallilizio, F. Levi. Phys. Rev. A, **66** (6), 063807 (2002).
[9] M.D. Lukin, A. Imamoğlu. Nature (London), **413**, 273 (2001).
[10] S.E. Harris. Phys. Lett., **62** (9), 1033 (1989).
[11] H.H. Jen, Daw-Wei Wang. Phys. Rev. A, **87** (6), 061802(R) (2013).
[12] C. Basler, J. Grzesiak, H. Helm. Phys. Rev. A, **92** (1), 013809 (2015).
[13] R. Liu, T. Liu, Y. Wang, Y. Li, B. Gai. Phys. Rev. A, **96** (5), 053823 (2017).
[14] Fam Le Kien, A. Rauschenbeutel. Phys. Rev. A, **91** (5), 053847 (2015).
[15] H.-H. Wang, J. Wang, Zh.-H. Kang, L. Wang, J.-Y. Gao, Y. Chen, X.-J. Zhang. Phys. Rev. A, **100** (2), 013822 (2019).
[16] M.J. Konopniki, J.H. Eberly. Phys. Rev. A, **24** (5), 2567 (1981).
[17] A. Rahman, J.H. Eberly. Phys. Rev. A, **58** (2), R.805 (1998).
[18] R. Grobe, J.H. Eberly. Laser Phys., **29** (3), 542 (1995).
[19] S.E. Harris, Zh.-F. Luo. Phys. Rev. A, **52** (2), R928 (1995).
[20] R. Grobe, F.T. Hioe, J.H. Eberly. Phys. Rev. Lett., **73** (24), 3183 (1994).
[21] V.G. Arkhipkin, I.V. Timofeev. Phys. Rev. A, **64** (5), 053811 (2001).
[22] A. Kasapi, M. Jain, G.Y. Yin, S.E. Harris. Phys. Rev. Lett., **74** (13), 2447 (1995).
[23] M. Jain, A. Kasapi, G.Y. Yin, S.E. Harris. Phys. Rev. Lett., **75** (4), 4385 (1995).
[24] O.M. Parshkov. Bull. Lebedev Phys. Institute, **49**, S43 (2022).
[25] P.A. Apanasevich. *Osnovy teorii vzaimodeystviya izlucheniya s veshchestvom* (Nauka i tekhnika, Minsk, 1977) (in Russian).
[26] R.L. de Zafra, A. Marshall. Phys. Rev., **170** (1), 28 (1968).
[27] I.S. Grigoryev, E.Z. Mejlikhov (red.). *Fizicheskie velichiny, Spravochnik.* (Energoatomizdat, M., 1991) (in Russian).
[28] S.L. McCall, E.L. Hahn. Phys. Rev., **183** (2), 457 (1969).
[29] A.N. Oraevsky. UFN, **168** (12), 1311 (1998). (in Russian).

Translated by EgoTranslating